

Supplementary Materials: HazeSpace2M: A Dataset for Haze Aware Single Image Dehazing

Anonymous Authors

Table 1: Descriptions of the notations used in Algorithm 1.

| Symbols | Description | Symbols | Description |
|----------|--------------------|----------------|------------------|
| Ω | Dataset | τ | Train dataset |
| ν | Validation dataset | ρ | Test dataset |
| ϕ | Dehazers | $\Delta\theta$ | Trained dehazers |
| C | Classifier | h_t | Haze type |
| I_h | Hazy input image | $J(x)$ | Dehazed image |
| δ | Modified ASM model | | |

1 PSEUDOCODE

Pseudocode of the Proposed Framework: In this paper, we propose a novel technique of specialized dehazers-based smart image dehazing based on the haze type classification. Algorithm 1 presents a step-by-step pseudocode of our proposed framework for processing a hazy image I_h to output the haze type h_t and the corresponding dehazed image $J(x)$. The algorithm requires a dataset Ω , a classifier C , and a set of trained dehazers $\Delta\theta$. The process begins by preparing the data, training a classifier on the dataset, classifying the type of haze present in the input image,



Figure 1: Sample images that we eliminated while collecting images for use as the GT images in the HazeSapce2M dataset. As these images contain different kinds of hazes, we eliminated them from the HazeSapce2M dataset.

Algorithm 1 Pseudocode of our proposed framework for haze aware single image dehazing.

```

1: Input: Hazy image  $I_h$ 
2: Outputs: Haze type  $h_t$ , Dehazed image  $J(x)$ 
3: Require:  $\Omega, C, \Delta\theta = \{\phi_{\text{cloud}}, \phi_{\text{EH}}, \phi_{\text{fog}}\}$ 
4: Data preparation:  $[\tau, \nu, \rho] = \text{split\_dataset}(\Omega)$ 

5: Procedure: TrainClassifier( $\tau$ )
6:   Train classifier  $C$  using dataset  $\tau$ 
7:   return  $C$ 
8: End Procedure

9: Procedure: ClassifyHazeType( $I_h, C$ )
10:   Haze type  $h_t \leftarrow C(I_h)$ 
11:   return  $h_t$ 
12: End Procedure

13: Procedure: PickDehazer( $h_t, \Delta\theta$ )
14:   Dehazer  $\delta \leftarrow$  select a dehazer from  $\Delta\theta$  based on  $h_t$ 
15:   return  $\delta$ 
16: End Procedure

17: Procedure: DehazeImage( $I_h, \delta$ )
18:   Dehazed image  $J(x) \leftarrow \delta(I_h)$ 
19:   return  $J(x)$ 
20: End Procedure

```

selecting an appropriate dehazer based on this classification, and finally applying the selected dehazer to produce a clear image.

Table 1 defines the symbols used in the algorithm, connecting the abstract symbols to their concrete meanings within the context of image dehazing. The table serves as a quick reference for understanding the variables and entities involved in the algorithm.

Together, the pseudocode and the table of notations provide a comprehensive overview of the proposed dehazing technique.

2 QUANTITATIVE ANALYSIS

As it is an extensive dataset, it is highly time-consuming to calculate the Peak Signal-to-Noise Ratio (PSNR) and Structural Similarity Index (SSIM) values for each hazy image. So, we separated 1,000 hazy images from level 1 to level 10 haze intensity as a sample and calculated the average PSNR and SSIM values for each subset and level. Table 2 and Table 3 compare image quality metrics, PSNR, and SSIM across different haze levels within the HazeSpace2M Dataset.

Average PSNR: Table 2 presents a comparative analysis of PSNR values across different haze intensities, offering an in-depth view of the image quality within the HazeSpace2M dataset. From left to right of the table, the haze intensity increases as the level increases, which is also evident by the average PSNR values of the images, considered here as a sample. It also breaks down the dataset by scene types (Outdoor, Street, Farmland, Satellite) and haze types (Fog, EH, Cloud), showing the impact of various haze levels on image clarity.

Table 2: Comparative analysis of PSNR across varying haze levels. This table details the PSNR values for different haze intensities (L1 to L10) within the HazeSpace2M dataset, divided by scene types (Outdoor, Street, Farmland, Satellite) and haze types (Fog, EH, Cloud). These metrics provide insights into the consistency of image quality amidst diverse hazy environments.

| Scene | Haze Type | Average PSNR for different levels of haze | | | | | | | | | |
|-----------|-----------|---|-------|-------|-------|-------|-------|-------|-------|-------|-------|
| | | L1 | L2 | L3 | L4 | L5 | L6 | L7 | L8 | L9 | L10 |
| Outdoor | Fog | 29.32 | 28.00 | 27.70 | 27.70 | 27.77 | 27.71 | 27.72 | 27.71 | 27.74 | 27.78 |
| | EH | 27.74 | 27.85 | 27.86 | 27.86 | 27.91 | 27.89 | 27.89 | 27.87 | 27.82 | 27.87 |
| Street | Fog | 30.53 | 29.49 | 28.95 | 28.63 | 28.45 | 28.37 | 28.20 | 28.20 | 28.16 | 28.17 |
| | EH | 27.68 | 27.72 | 27.86 | 27.92 | 27.84 | 27.78 | 27.76 | 27.82 | 27.87 | 27.79 |
| Farmland | Fog | 29.67 | 28.26 | 27.82 | 28.26 | 27.82 | 27.80 | 27.75 | 27.76 | 27.80 | 27.85 |
| | EH | 27.70 | 27.77 | 27.87 | 27.92 | 27.96 | 27.92 | 27.89 | 27.88 | 27.82 | 27.80 |
| Satellite | Cloud | 29.67 | 29.49 | 27.58 | 27.49 | 27.63 | 27.72 | 27.87 | 27.99 | 28.07 | 28.11 |
| Average | | 28.90 | 28.37 | 27.95 | 27.97 | 27.91 | 27.88 | 27.86 | 27.89 | 27.89 | 27.91 |

Table 3: Evaluation of image quality across haze intensity levels. This table shows average SSIM scores for different levels of haze (L1 to L10) within the HazeSpace2M dataset across various scenes (Outdoor, Street, Farmland, Satellite) and corresponding haze types (Fog, EH, Cloud), illustrating the dataset’s utility for image quality assessment under varying hazy conditions.

| Scene | Haze Type | Average SSIM for different levels of haze | | | | | | | | | |
|-----------|-----------|---|------|------|------|------|------|------|------|------|------|
| | | L1 | L2 | L3 | L4 | L5 | L6 | L7 | L8 | L9 | L10 |
| Outdoor | Fog | 0.97 | 0.94 | 0.83 | 0.83 | 0.79 | 0.71 | 0.68 | 0.66 | 0.64 | 0.60 |
| | EH | 0.96 | 0.91 | 0.83 | 0.81 | 0.77 | 0.73 | 0.70 | 0.65 | 0.63 | 0.59 |
| Street | Fog | 0.98 | 0.97 | 0.94 | 0.90 | 0.86 | 0.79 | 0.74 | 0.74 | 0.67 | 0.63 |
| | EH | 0.96 | 0.91 | 0.84 | 0.82 | 0.78 | 0.74 | 0.70 | 0.66 | 0.65 | 0.60 |
| Farmland | Fog | 0.97 | 0.94 | 0.56 | 0.94 | 0.56 | 0.51 | 0.67 | 0.64 | 0.61 | 0.57 |
| | EH | 0.94 | 0.88 | 0.79 | 0.76 | 0.72 | 0.68 | 0.64 | 0.61 | 0.56 | 0.51 |
| Satellite | Cloud | 0.97 | 0.98 | 0.94 | 0.85 | 0.76 | 0.72 | 0.66 | 0.60 | 0.56 | 0.52 |
| Average | | 0.96 | 0.93 | 0.82 | 0.84 | 0.75 | 0.70 | 0.68 | 0.67 | 0.62 | 0.57 |

This table is a testament to the dataset’s comprehensive nature and applicability in assessing image quality in hazy conditions.

Average SSIM: Table 3 further complements this by providing average SSIM scores for the same levels of haze intensity, scene, and haze types. SSIM scores provide insight into the perceived quality of images, highlighting the dataset’s utility for more subjective assessments of image quality under varying hazy conditions. These metrics collectively underscore the dataset’s robustness for developing advanced dehazing algorithms.

3 QUALITATIVE ANALYSIS

We assured the quality of the GT images while picking them from various sources, as also mentioned in Section 3.1 of the paper. For example, we eliminated the images from the SOTS [1] dataset, finding the images with hazes present in them. Figure 1 shows some hazy images that we found during data collection, which were disqualified to be the GT images of the HazeSapce2M dataset.

Figure 2 offers a visual range of haze intensities within the HazeSpace2M dataset, showcasing images that progressively intensify in the haze. This array of images vividly demonstrates the range of visibility reduction across various environmental conditions, including outdoor scenes, streets, farmlands, and satellite views. Each

row corresponds to a different subset, with the transition from left to right depicting a gradual increase from clear to heavily hazed images. The gradation serves as a crucial reference for developing and testing dehazing algorithms, enabling a nuanced understanding of how different haze levels affect image perception. This representation underscores the dataset’s versatility and richness, making it a valuable resource for researchers aiming to improve image clarity in diverse atmospheric conditions. The visual gradation also highlights the dataset’s potential to train models that can accurately classify haze types. This ensures optimal image enhancement in a wide range of real-world multimedia applications.

We found the ResNet50 model to give the best accuracy, as discussed in Section 5.1 when evaluating against the synthetic benchmarking datasets and the real hazy image dataset for classifying the haze type presented in a single input image. Figure 3(a) reveals the training and validation loss curves for the ResNet50 model. These curves illustrate a decrease in validation loss relative to training loss over time. Additionally, the figure indicates that the model’s training was halted after 35 epochs using the early stopping technique. The confusion matrix for the same model is also presented in Figure 3(b), which shows that even though the model classifies the Cloud-type haze with higher accuracy, it struggles to classify the two other hazes, namely Fog and EH. The confusion matrix and the

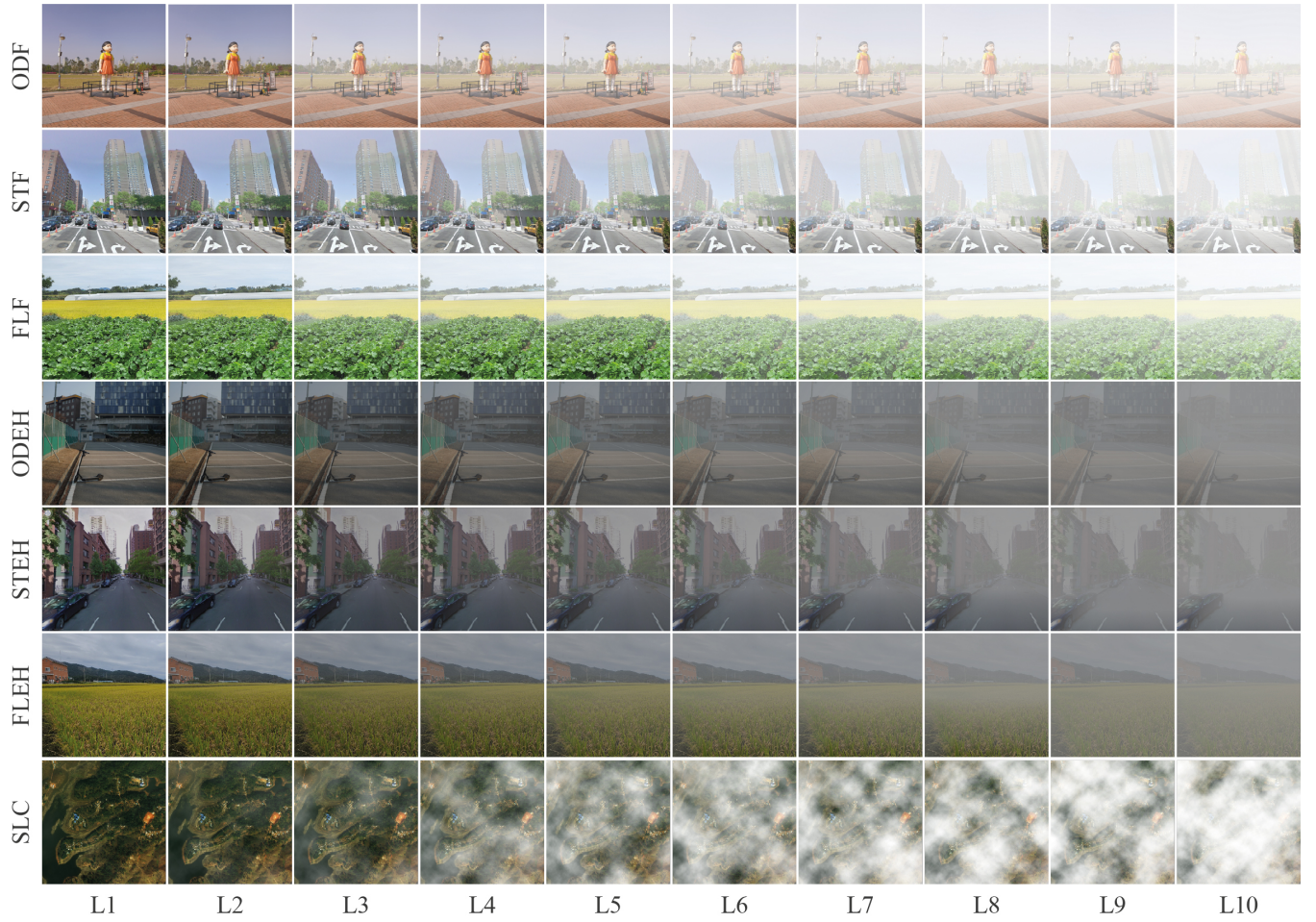


Figure 2: Examples of haze intensities across different scene types within the HazeSpace2M dataset. Each row represents a subset (Outdoor, Street, Farmland, and Satellite) with images transitioning from low to high haze levels, following the order of left to right. To avoid repetition, abbreviations used in this figure are not defined and are given in Table 3 of the main paper.

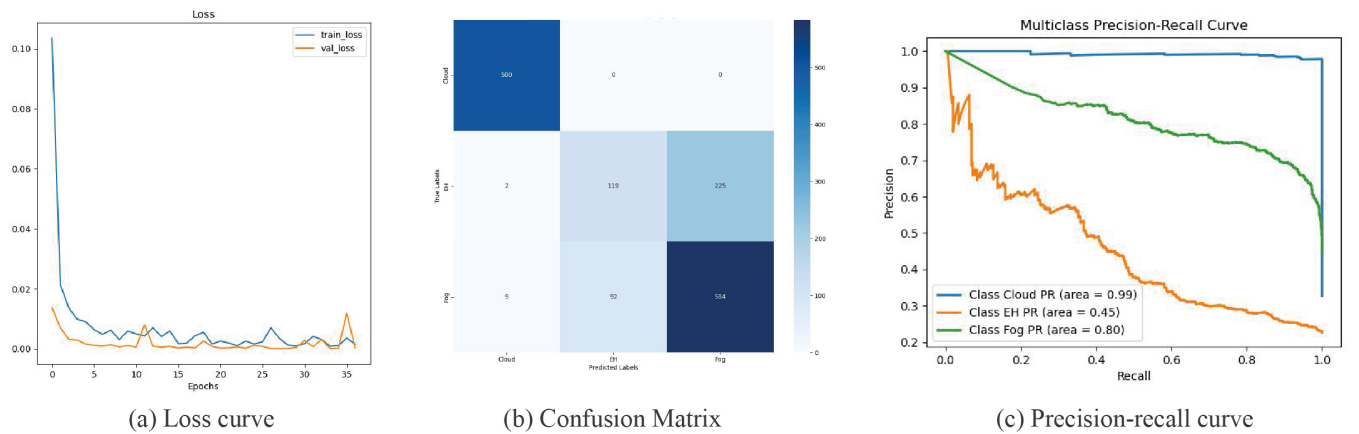


Figure 3: (a) Train and validation loss curve for training the ResNet50 model, (b) Confusion matrix of ResNet50, and (c) Precision-recall curve of the same model while evaluating it on the Real Hazy Testset (RHT) of the HazeSpace2M dataset. ResNet50 is selected as a sample because its result is the highest on the RHT.

precision-recall curve are presented in Figure 3(b & c), showing that some of the hazes were classified as EH while they were actually Fog and vice versa. This is because of the nature of the hazes. In reality, the EH and Fog-type hazes are quite similar, validating the challenges in classifying haze types in real images.

REFERENCES

[1] Boyi Li, Wenqi Ren, Dengpan Fu, Dacheng Tao, Dan Feng, Wenjun Zeng, and Zhangyang Wang. 2018. Benchmarking single-image dehazing and beyond. *IEEE Transactions on Image Processing* 28, 1 (2018), 492–505.